Jurnal Teknologi

Full paper

Assessment of Green Inhibitor on the Crystal Structures of Carbonated Concrete

Abdulrahman, A. S.[a*], Mohammad Ismail[b]

[a]*Department of Mechanical Engineering, Federal University of Technology PMB 65, Minna, Nigeria*
[b]*UTM Construction Research Centre, Faculty of Civil Engineering, Universiti Teknologi Malaysia, 81310 UTM Johor Bahru, Johor, Malaysia*

*Corresponding author: asipita.salawu@futminna.edu.ng

Article history

Received :10 March 2014
Received in revised form :
28 April 2014
Accepted :15 May 2014

Graphical abstract

Abstract

The present paper involves studies of inhibitors on carbonation depth and carboaluminates of concrete which was exposed to accelerated carbonation. Three inhibitors used were; calcium nitrite, ethanolamine and eco-friendly green *Bambusa Arundinacea*. Concrete mix was designed to be 30 MPa with 0.45 W/C ratios which was chloride contaminated by 1.5% weight of cement content from analytical grade of magnesium chloride salt. Inhibitors additions were 2% and 4% weight of cement content. The results show that *Bambusa arundinacea* inhibitor distinctively shows lowest level of carbonation. This developed hydrophobic green inhibitor characteristics was able to form impermeable barrier against CO_2 gas. Additionally, hemicarboaluminate phases appears at hydration in calcite-containing Portland cement, even in the presence of two inhibitors (calcium nitrite and ethanolamine) which gradually converted to monocarboaluminate. Whereas, *Bambusa arundinacea* inhibitor causes the saturation of portlandite that maintained Ca/Si ratio above 1.65 and C-S-H remain unaffected by carbonation.

Keywords: Concrete; carbonation; inhibitors; durability; AFm phases

1.0 INTRODUCTION

Cements are one of the most used materials in the construction industry and civil engineering. Carbonation of concrete is associated with the corrosion of steel reinforcement and concrete durability [1]. Carbonation occurs when carbon dioxide in the atmosphere in the present of moisture reacts with the products of concrete hydration especially calcium hydroxide, calcium silicate hydrates and calcium aluminate to form carbonates, e.g. calcite and aragonite, while other cement compounds are carbonated to AFm phases (hemicarboaluminate and monocarboaluminate) [2, 3]. These carbonation reactions depassivate high alkali concrete pH to drastically drop from about 12.5-13 to 8.5-9, resulting into dusty weak surfaces. The lowest level for concrete durability, when subjected to a carbonation environment, is often referred to as the state that carbonation reaches the depth of the steel, in which steel starts to corrode then to reduce dramatically the performance of concrete structures. Carbonate-containing AFm phases are mainly formed during the carbonation process of many different building materials.

The AFm phases are hydrated tetracalcium aluminate compounds belonging to the lamellar double hydroxide (LDH) family. They occur during the hydration process of many kinds of cement. AFm phases are composed of positively charged main layer $[Ca_2Al(OH)_6]^+$ and negatively charged interlayer $[X.nH_2O]^-$ where X is either one monovalent anion or half a divalent anion. The following general formulae $3CaO.Al_2O_3.CaX_2.nH_2O$ for monovalent anions or $3CaO.Al_2O_3.CaX.nH_2O$ for divalent anions are generally used in cement chemistry [4, 5, 6].

Glasser and Matschei [7] reported that AFm phases is believed to be an important "sink" for chloride ions migration into concrete, which accelerate corrosion of embedded steel. So, previous work on effect of CO_2 on AFm phases was handicapped as a result of difficulty of preventing progressive carbonation and controlling the activity, a, of CO_2. Therefore, the present study concentrates on carbonation of inhibited concrete and its effect on the structures.

2.0 EXPERIMENTAL PROCEDURE

2.1 Materials

Ordinary Portland Cement (OPC) was used in this work. Coarse aggregates of size 20 mm and 10 mm of quartzite origin were used in the ratio of 1.78:1 to satisfy the overall grading requirement of coarse aggregate in accordance with ASTM C192.

Land quarried sand satisfying BS 882:1992 was used as fine aggregate. The sand has a fineness modulus of 2.5. Tap water was used for the preparation of specimens. All the concrete mixes were designed for similar workability with slump of 30–60 mm. The water content was kept constant to 230 kg/m^3 for the desired slump in all the mixes to have similar workability. The water–cement ratio (w/c) used was 0.45. The fresh density of concrete was then obtained as per guidelines specified by British method of mix selection (DOE) to be 2380 Kg/m^3. The mix design was similar to a companion paper published by Asipita *et al*. [9].

2.2 Carbonation Test

The carbonation depth measurement test was performed in accordance with method used by [10, 11, 12]. Specimens were accelerated carbonated by exposing them to an atmosphere of 65-75 relative humidity (RH) in sealed plastic tanks through which CO_2 gas was passed for about 30min, twice per day at 25-30^{0}C. The pressure inside the curing chamber was monitored by a pressure gauge attached on the curing chamber. After the designed pre-conditioning period, the specimens were put into the curing chamber for CO_2 curing. Then the curing chamber with specimens was closed, vacuumed to a pressure of around 600 mm Hg and maintained for 2 min before CO_2 was injected. The CO_2 pressure used for curing was 20 Psi. The pressure of CO_2 inside the chamber was controlled by a regulator on the CO_2 tank. After two month of this treatment, the specimens were tested for carbonation by the phenolphthalein test.

Phenolphthalein was prepared as 1% solution by dissolving 1mg of phenolphthalein powder indicator in 90cc of 2-propanol (iso-propanol). The solution was made up to 100cc by adding distilled water. On freshly extracted cores, it was sprayed with phenolphthalein solution on a split core; the depth of the uncolored layer (the carbonated layer) from the external surface was measured to the nearest mm at four positions, and average taken. When 1% of phenolphthalein solution is applied to normal concrete, it will turn bright pink. If the concrete has undergone carbonation, no colour change will be observed [13].

2.3 Field Emission Scanning Electron Microscopy (FESEM)

Field Emission Scanning Electron Microscopy (FESEM) was used for the micro-structural analysis of the steel embedded in concrete and concrete morphology. The analyzer was fitted with energy dispersive X-ray detector (EDX) for elemental analysis. Three points were considered for elemental composition and then the average values are reported.

■3.0 RESULTS AND DISCUSSIONS

3.1 Carbonation Depth

At the end of exposure to CO_2, samples were cored and split into two pieces where phenolphthalein indicator was sprayed for carbonation depth measurement. Carbonation depth was determined as the distance between the external surface of the concrete and the end of the coloured region. Colour changes were observed for ten seconds to ascertained true carbonation. A reddish-purple (pink) colour indicate absents of carbonation, while colourless portion signifies carbonation effect. Meanwhile partial carbonation do occur which shows faint pink colour.

Figures 1-4 shows accelerated carbonated samples of 1.5% $MgCl_2$ contamination and 2% and 4% of various inhibitors additions. Their carbonation depths are presented in bar chart format as shown in Figure 6. According to this Figures, depths of carbonation has tendency to increase with progress of accelerated curing regardless of inhibitors. But outstandingly, *Bambusa arundinacea* distinctively shows lowest level of carbonation. This developed hydrophobic green inhibitor characteristics was able to form impermeable barrier against CO_2 gas as indicated in Figure 5. Also the high level of carbonations of $Ca(NO_2)_2$ inhibited samples is not surprising, even above the chloride contaminated sample as shown in Figures 3. Ngala *et al*. [14] observed that nitrite inhibitor admixture to concrete has not been found to function effectively in a carbonated concrete with significant chloride contamination. As nitrite is an anodic inhibitor, its mechanism of corrosion rate limitation in carbonated concrete that contains chloride ions involves anodic resistance control, which hindered ionic migration in the vicinity of anodic sites. So, it easy for CO_2 gas to penetrate the structure and alter the alkalinity pH level from 13 to 9, as evident in the faint pink colour of the entire structure.

The effects of ethanolamine inhibitor to prevent accelerated carbonation are shown in Figure 4. Though the carbonation depth is lower than the chloride contaminated sample, but not as compared to *Bambusa arundinacea* inhibitor. Sawada *et al*. [15] suggested reasons while ethanol amine inhibitor is not effective in checking carbonation. They reasoned that when ethanolamine cations migrate through the thoroughly carbonated concrete in which the pore solution pH is generally less than 9.5, and then deprotonation occurs, which causes loss of alkali accumulation in the molecular form ahead of the cathode. It's the accumulation of ethanolamine that creates a steep concentration gradient that protects steel reinforcement in concrete.

Figure 1 Accelerated carbonated of control

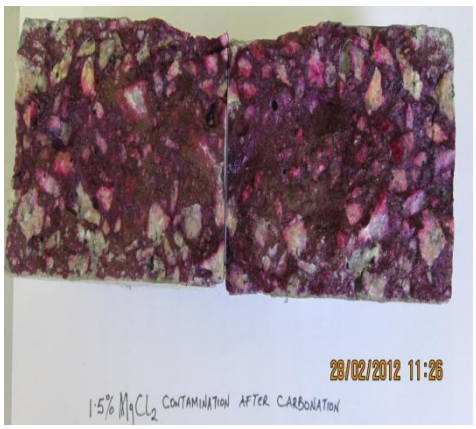

Figure 2 Accelerated carbonated of 1.5% $MgCl_2$ contaminated sample

(a) (b)

Figure 3 Accelerated carbonation for 2% (a) and 4% (b) $Ca(NO_2)_2$ inhibited sample for 0.45w/c of 1.5% $MgCl_2$ contamination

(a) (b)

Figure 4 Accelerated carbonation for 2% (a) and 4% (b) C_2H_7NO inhibited sample for 0.45w/c of 1.5% $MgCl_2$ contamination.

(a) (b)

Figure 5 Accelerated carbonation for 2% (a) and 4% (b) *Bambusa* inhibited sample for 0.45w/c of 1.5% $MgCl_2$ contamination.

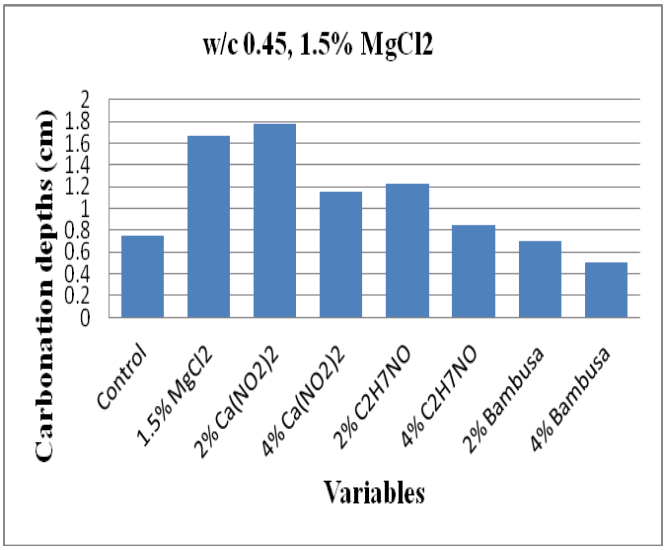

Figure 6 Carbonation depths of accelerated carbonated samples for 1.5% $MgCl_2$ contamination of 0.45w/c

In general, the carbonation depths can be related to the time for the CO_2 gas to penetrate the concrete cover to the level of steel reinforcement. This is governed by Fick's first law of diffusion expressed as follows:

$$X = K(t)^{0.5}$$

Where, X is the carbonation depth (cm), t is exposure time (years) and K is the carbonation coefficient (cm/years$^{0.5}$) according to Valcuende and Parra [16]. In this work, we design for 30 MPa grade concrete with 25 mm cover depth. By this design thickness, the time required for carbonation to reach reinforcement level will be 25 years life span. Consequently, carbonation time was calculated for all the samples using the above formula. Time to carbonation in years was plotted on bar chart for ease of discussions. The results are shown in Figure 7.

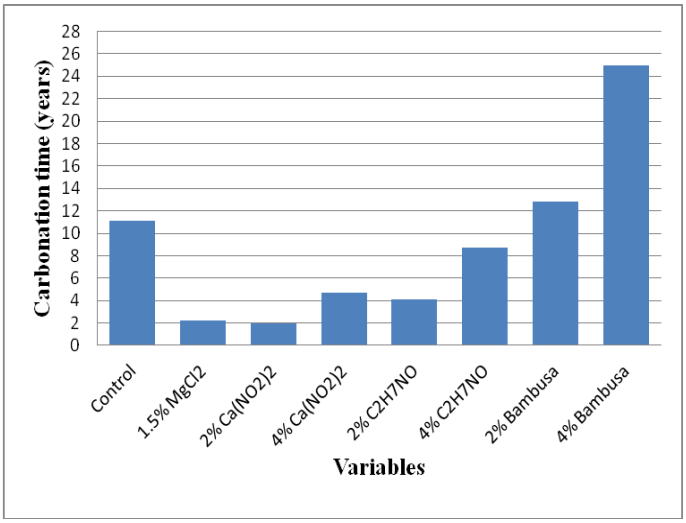

Figure 7 Time required for accelerated carbonation for 0.45w/c, 1.5% $MgCl_2$ addition to concrete

3.2 AFm Phases

The carbonated control sample in Figure 8 shows decomposed hemicarboaluminate from AF_m phases to stable calcite. This is as a result of depletion of portlandite by carbonation that causes low Ca/Si ratios in C-S-H. Glasser and Matschei [7] suggested that once a Ca/Si ratio is less than 1.3 in C-S-H, the carbonated structure formed is a stable calcite. Also the chloride contaminated sample in Figure 9 shows the formations of brucite as a result of high magnesium ions (white background) and ettringite which cause cracks as noticed in the structure. The magnesium ion reacts with portlandite and diminishes it rapidly, leaving unstable C-S-H structure that transformed into ettringite.

Previous research shows that the AFm phases play a key important role with respect to the interactions with carbonation. So, Figures 10-11 shows a mixture of $Al(OH)_3$ and monocarboaluminate ($C_4A\acute{C}H_{11}$) as a result of carbonation preferentially attack on C-S-H structure while portlandite still remains in the pores. This can be attributed to the high aluminium content and Ca/Si ratio as summarized in Table 1. The AFm phases formed during hydration from monosulfoaluminate ($C_4A\acute{S}H_{12}$) was partially replaced by hydroxyl from $Al(OH)_3$. This type of AF_m phase's transformations was similarly observed in the work of Ipavec *et al*. [17]. Conversely, ethanolamine inhibited samples in Figures 12-13 shows a complete depleted portlandite and formation of strätlingite (C_2ASH_8) from alumina released by the decomposition of monocarboaluminate from C-S-H. Consequently, this structure contains calcite, $Al(OH)_3$ and strätlingite as was similarly observed in a previous research by Glasser and Matschei [7]. Also developed *Bambusa arundinacea* inhibitor in Figures 14-15 consists mainly of C-S-H, portlandite and a monosulfoaluminate-type AFm-phase at the earliest stages of carbonation. As the rate of carbonation increases, monosulfoaluminate might decompose to hemicarbonate and monocarbonate that forms ettringite. Although is difficult to convoluted from other AFm phases. According to Glasser and Matschei [7] once the saturation of portlandite is maintained within Ca/Si of 1.65 and above, the C-S-H remain unaffected by carbonation. Whereas, once the portlandite is depleted, the Ca/Si ratio of C-S-H decreases progressively from 1.65 to 0.8. Albeit, the structures in this Figures 14-15 is not necessarily immutable to decalcification and ettringite formations: phase's changes can reconstitute the microstructure, therefore cracks initiation can be observed in the micrographs.

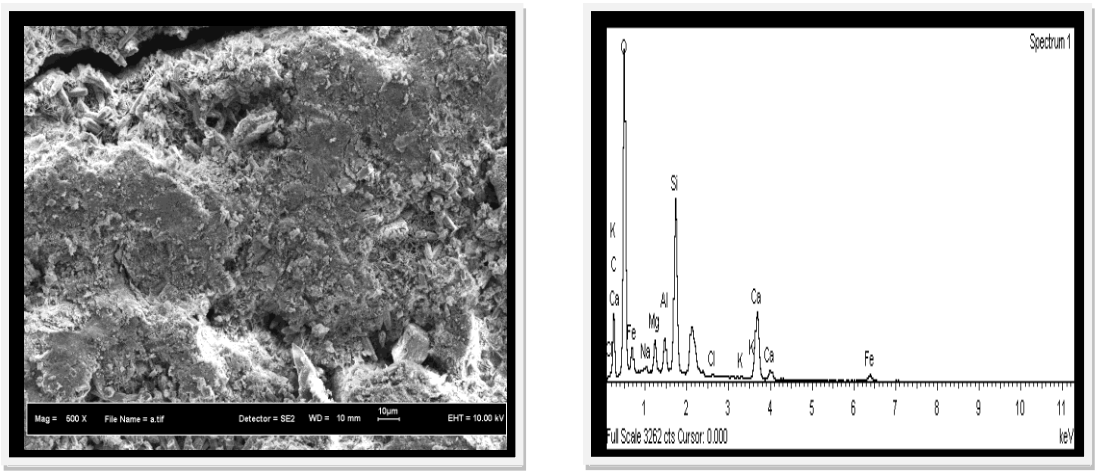

Figure 8 FESEM/EDX image of carbonated control sample (0.45w/c)

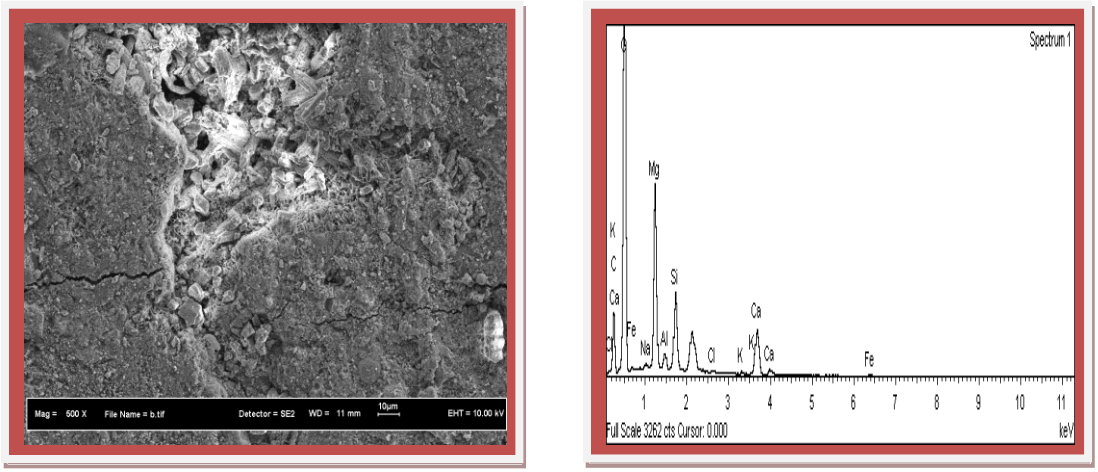

Figure 9 FESEM/EDX image of carbonated 1.5% $MgCl_2$ contaminated sample

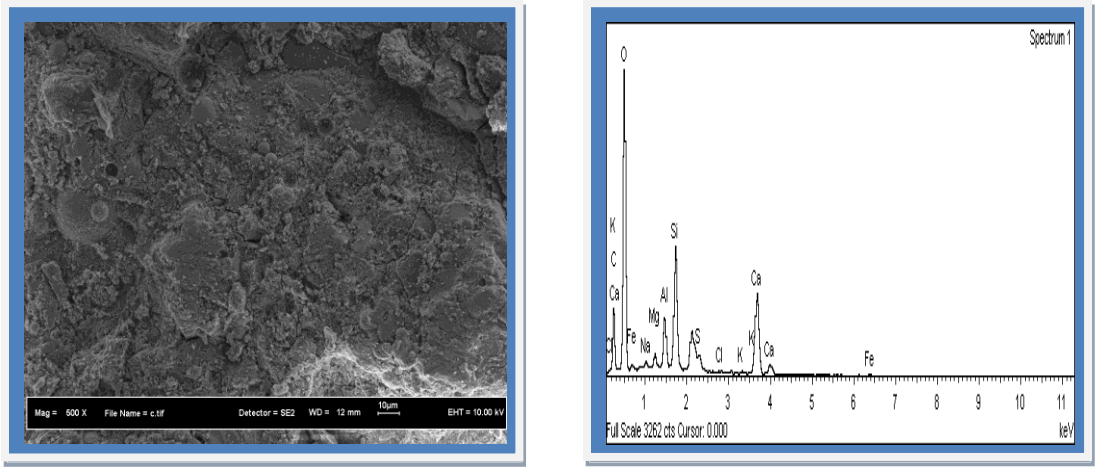

Figure 10 FESEM/EDX image of carbonated 2% $Ca(NO_2)_2$ inhibited sample

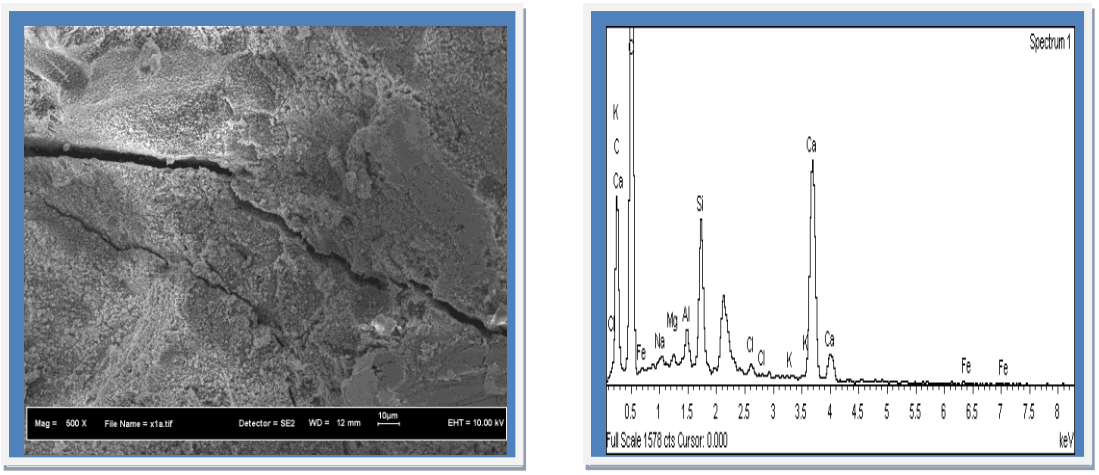

Figure 11 FESEM/EDX image of carbonated 4% $Ca(NO_2)_2$ inhibited sample

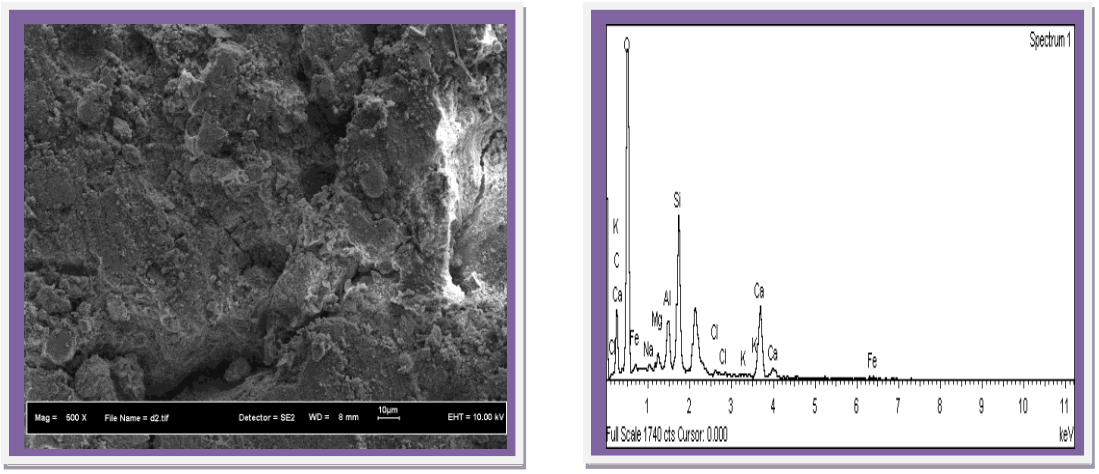

Figure 12 FESEM/EDX image of carbonated 2% C_2H_7NO inhibited sample

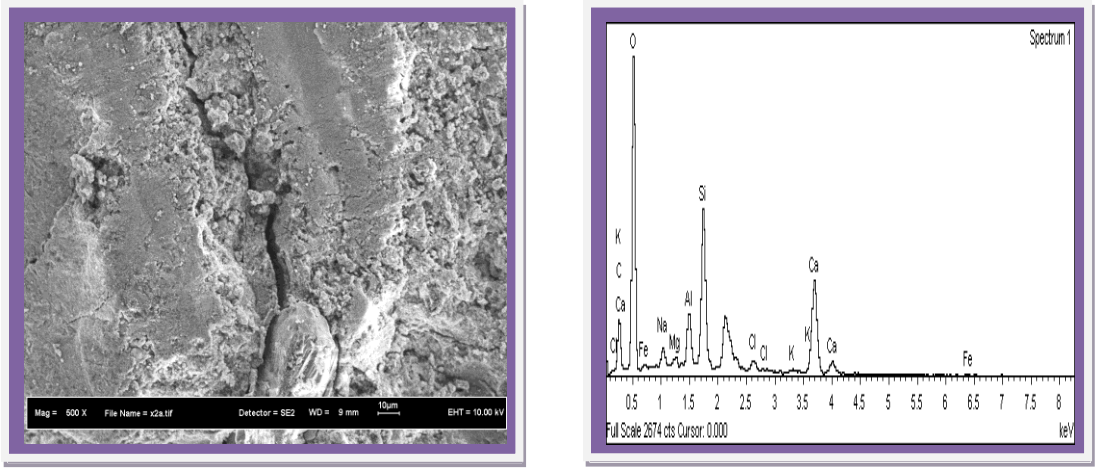

Figure 13 FESEM/EDX image of carbonated 4% C_2H_7NO inhibited sample

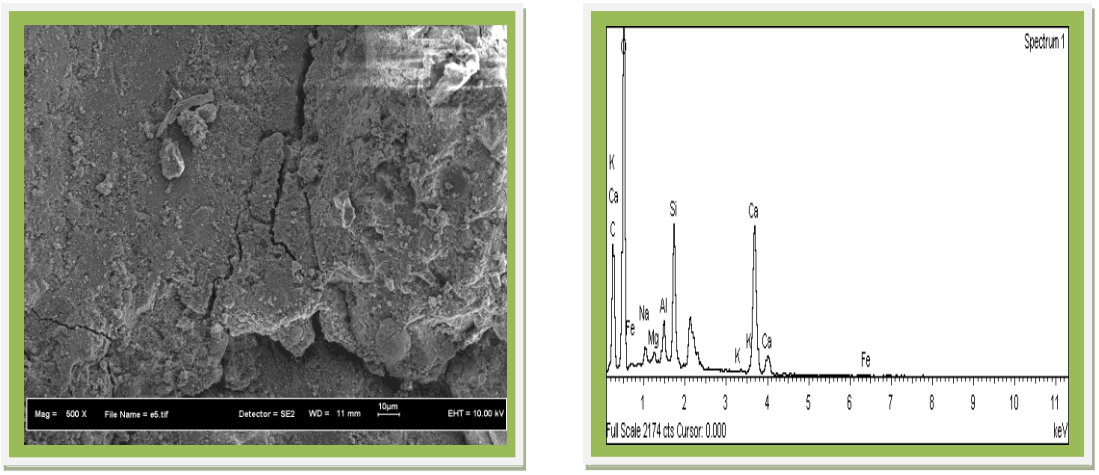

Figure 14 FESEM/EDX image of carbonated 2% Bambusa inhibited sample

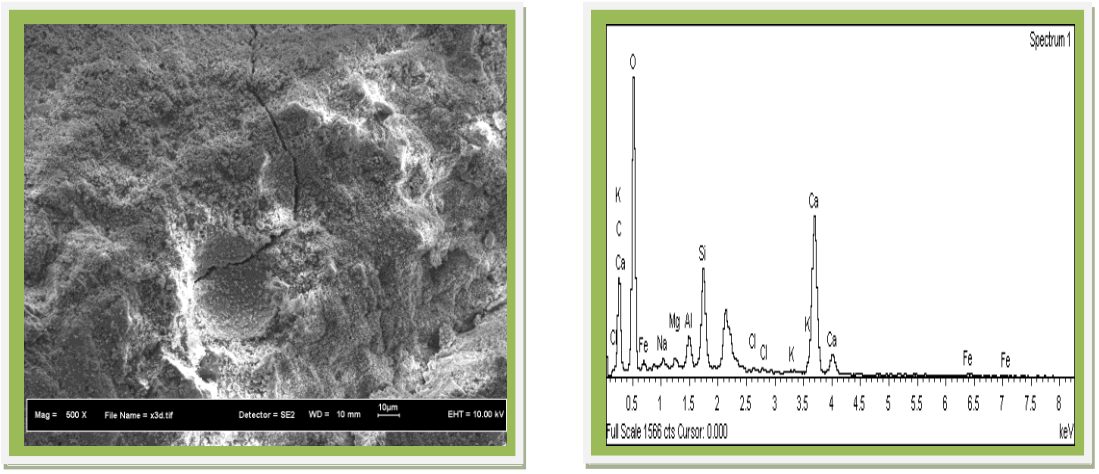

Figure 15 FESEM/EDX image of carbonated 4% Bambusa inhibited sample

4.0 CONCLUSIONS

Bambusa arundinacea inhibitor could salvage the concrete to meet its designed life cycle, as its time to accelerated carbonate is 25 years. *Bambusa arundinacea* green inhibitor reduced chloride ion diffusivity which reduces internal transition zone (ITZ) percolation and it enhanced cement hydration due to internal curing effects from the inhibitors leading to reduced capillary pores as a result of residual alkalinity of potassium hydroxide (KOH) present in the concrete. KOH provides new nucleation sites for calcium carboaluminates as results of the reaction between $CaCO_3$ and C_3A from Portland clinker.

The depths of carbonation has tendency to increase with progress of accelerated curing regardless of inhibitors. But outstandingly, *Bambusa arundinacea* distinctively shows lowest level of carbonation. This developed hydrophobic green inhibitor characteristics was able to form impermeable barrier against CO_2 gas penetration.

$Ca(NO_2)_2$ inhibited samples shows the high level of carbonations as a result of significant chloride contamination as nitrite is an anodic inhibitor, its mechanism of corrosion rate limitation in carbonated concrete that contains chloride ions involves anodic resistance control, which hindered ionic migration in the vicinity of anodic sites.

Ethanolamine inhibitor is not effective in checking carbonation because of its deprotonation, which causes loss of alkali accumulation in the molecular form ahead of the cathode. It's the accumulation of ethanolamine that creates a steep concentration gradient that protects steel reinforcement in concrete.

References

[1] Jack, M. C., R. Huang, and C. C. Yang. 2002. Effects of Carbonation on Mechanical Properties and Durability of Concrete Using Accelerated Testing Method. *Journal of Marine Science and Technology*. 10(1): 14–20.

[2] Tomce, R., E. D. Robert, V. M. Oxana and P. Herbert. 2012. Crystal Structure of Calcium Hemicarboaluminate and Carbonated Calcium Hemicarboaluminate from Synchrotron Powder Diffraction Data. *Acta Crytals*. B68: 493–500.

[3] Raafat, E. H., M. Amir, A. Cook and S. Rizkalla. 2011. Effectiveness of Surface-applied Corrosion Inhibitors for Concrete Bridges. *Journal of Materials in Civil Engineering*. 271–280.

[4] Mesbah, A., J-P. Rapin, M. Francios, C. Cau-dit-Coumes, F. Frizon, F. Leroux and G. Renaudin. 2011a. Crystal Structures and Phase Transition of Cementitious Bi-Anionic AFm-(Cl^-, CO_3^{2-}) Compounds. *Journal of American Ceramic Society*. 94(1): 261–268.

[5] Bonavetti, V. L., V. F.Rahhal and E. F. Irassar. 2001. Studies on the Carboaluminate Formation in Limestone Filler-blended Cements. *Cement and Concrete Research*. 31: 853–859.

[6] Mesbah, A., C. Cau-dit-Coumes, F. Frizon, F. Leroux, J. Ravaux and G. Renaudin. 2011b. A New Investigation of the Cl^-- CO_3^{2-} Substitution in AFm Phases. *Journal of American Ceramic Society*. 94(6): 1901–1910.

[7] Glasser, F.P. and T. Matschei. 2009. *Interactions between Cement and Carbondioxide*. University of Aberdeen, Old Aberdeen, AB24 3UE Scotland, UK.

[8] American Society for Testing and Materials, 2007. *ASTM C192. Standard Practice for making and Curing Concrete Test Specimens in the Laboratory*. West Conshohocken, PA.

[9] Asipita, S. A., M. Ismail, M. Z. A. Majid, Z.A. Majid, C. S. Abdullah and J. Mirza. 2014. Green *Bambusa Arundinacea* Leaves Extract as a Sustainable Corrosion Inhibitor in Steel Reinforced Concrete. *Journal of Cleaner Production*. 67: 139–146.

[10] Sawada, S. K., C. L. Page and M. M. Page. 2005. Electrochemical Injection of Organic Corrosion Inhibitors into Concrete. *Corrosion Science*. 47(8): 2063–2078.

[11] Ngala, V. T., C. L. Page and M. M. Page. 2003. Corrosion Inhibitor Systems for Remedial Treatment of Reinforced Concrete. Part 2: Sodium Monofluorophosphate. *Corrosion Science*. 45: 1523–1537.

[12] Page, M.M., C. L. Page, V. T. Ngala, and D.J. Anstice. 2002. Ion Chromatographic Analysis of Corrosion Inhibitors in Concrete. *Construction and Building Materials*. 16(2): 73–81.

[13] Shi, C., F. He and Y. Wu. 2012. Effect of Pre-conditioning on CO_2 Curing of Lightweight Concrete Blocks Mixtures. *Construction and Building Materials*. 26(1): 257–267.

[14] Ngala, V. T., C. L. Page and M. M. Page. 2002. Corrosion Inhibitor Systems for Remedial Treatment of Reinforced Concrete. Part 1: Calcium Nitrite. *Corrosion Science*. 44(9): 2073–2087.

[15] Sawada, S. K., C. L. Page and M. M. Page. 2007. Electrochemical Injection of Organic Corrosion Inhibitors into Carbonated Cementitious Materials: Part 1. Effects on Pore Solution Chemistry. *Corrosion Science*. 49(3): 1186–1204.

[16] Valcuende, M. and C. Parra. 2010. Natural Carbonation of Self-compacting Concretes. *Construction and Building Materials*. 24: 848–853.

[17] Ipavec, A., R. Gagrovsek, T. Vuk, V. Kaucic, J. Macek, and A. Meden. 2011. Carboaluminate Phases Formation During the Hydration of Calcite-containing Portland Cement. *Journal of American Ceramic Society*. 94(4): 1238–1242.

Table 1 Summary of energy dispersive x-ray spectroscopy (EDX) results for accelerated carbonated concrete samples at w/c 0.45

Samples	Element average weight (%)											Ca/Si ratio
	C	O	Al	Si	Cl	Ca	Mg	Na	K	Fe	S	
Control (0.45w/c)	11.84	39.68	2.24	12.40	0.22	15.75	1.93	0.24	0.23	15.17	-	1.27
Control (0.65w/c)	12.74	46.48	1.22	6.16	0.91	17.64	9.16	0.05	0.35	5.24		2.86
1.5% $MgCl_2$ contaminated	12.10	52.45	1.18	6.19	0.17	11.77	12.08	0.27	0.46	3.33	-	1.90
4.5% $MgCl_2$ contaminated	12.07	49.28	2.52	8.10	0.35	21.02	2.01	0.27	0.22	4.16		2.60
2% $Ca(NO_2)_2$	11.83	46.90	3.52	9.86	0.09	21.63	0.82	0.46	0.17	3.90	0.7	2.19
4% $Ca(NO_2)_2$	12.38	49.36	1.05	5.56	0.75	28.73	0.39	0.26	0.05	1.47	-	5.17
2% C_2H_7NO	13.15	47.16	3.18	11.94	0.43	18.39	0.95	0.45	0.21	4.14	-	1.54
4% C_2H_7NO	9.41	46.13	3.40	11.42	1.62	22.67	0.48	1.23	0.51	3.13	-	1.99
2% *Bambusa*	13.56	47.38	1.86	7.47	-	26.42	0.37	0.76	0.09	2.10	-	3.54
4% *Bambusa*	11.01	41.86	1.73	6.01	1.33	31.79	0.49	0.44	0.23	6.11	-	5.29